Pure & Appl. Chem., Vol. 69, No. 12, pp. 2541–2565, 1997.
Printed in Great Britain.

INTERNATIONAL UNION OF PURE
AND APPLIED CHEMISTRY

MACROMOLECULAR DIVISION
COMMISSION ON POLYMER CHARACTERISATION AND PROPERTIES
WORKING PARTY ON STRUCTURE AND PROPERTIES OF COMMERCIAL POLYMERS*

CHARACTERISATION OF FINITE LENGTH COMPOSITES: Part VI—Rheological studies of materials based on the polypropylene matrix

(Technical Report)

Prepared for publication by

R. S. BAILEY‡ AND D. J. GROVES

‡address for correspondence: ICI Technology, P.O. Box 90, Wilton, Middlesbrough, Cleveland TS90 8JE, UK

*Contributing Members of the Working Party during the period 1989–93 in which this report was prepared was principally as follows:

Chairman: D. R. Moore (UK); ***Secretary:*** H. M. Laun (Germany); ***Members:*** G. Ajroldi (Italy); R. S. Bailey (UK); J. Curry (USA); C. Dehennau (Belgium); M. Fleissner (Germany); A. Ghijsels (Netherlands); W. Gleissle (Germany); D. J. Groves (UK); J. Lawler (USA); J. Lyngaae-Jorgensen (Denmark); J. Meissner (Switzerland); A. Plochocki (USA); L. A. Utracki (Canada); G. Vassilatos (USA).

Characterisation of finite length composites: Part VI—Rheological studies of materials based on the polypropylene matrix (Technical Report)

R. S. Bailey‡ and D. J. Groves
‡ICI Technology, P. O. Box 90, Wilton, Middlesbrough, Cleveland TS90 8JE, UK

Abstract: A range of rheological and morphological techniques, contributed by nine laboratories, are used to characterise the flow behaviour in a model long fiber reinforced thermoplastic system. It is concluded that in capillary rheometry, the pressure drop fluctuations that typify the flow arise from two mechanisms, that of local fiber fraction inhomogeneity passing through the die, and the instability of the vortices in the die entry region which worsen as shear rate is increased. It is clear that the test geometry is significant in both capillary and torsional measurements. Yield stresses of 3.5 Pa (5 mm fiber length) and 7 Pa (10 mm fibres) have been evaluated.

1. INTRODUCTION

The materials under study are commercially available as pultrusion compounded injection moulding compounds and are known as long fiber reinforced thermoplastics. These materials offer an increased precursor fiber length over their conventional extrusion compounded counterparts. The granular feedstock for these materials is highly anisotropic with bundles of fibres aligned along the granule axis. After flow through nozzle, runner and gates in an injection moulding machine, the fibres become more uniformly dispersed in the mould cavity. The fibres are oriented more randomly in the moulded part, to the extent that controlled pyrolysis of the matrix polymer in a component may leave the shape retained by the residual fiber skeleton intact. The rheology in the mould cavity, therefore, differs from that of the feedstock. Some aspects of the rheology of this class of mouldable thermoplastic fiber composite have been reported by Gibson (1) and Gibson, Corscadden and McClelland (2) using an instrumented moulding machine nozzle; fiber bundles are still observed in polymer taken from the nozzle region in spite of the preshearing history. It is now a requirement for materials selection that an understanding of both high shear rate and in-cavity rheology is established for design practices. This places a requirement for at least a reproducible flow curve to be available, which can be fitted by a simple curve fit for injection mould filling simulation software.

Converging flow in the entry into a die or gate is expected to be particularly important with high Trouton ratios of about 100 reported for a long fiber moulding compound by Gibson (3) and Gibson and Williamson (4). For long glass fiber in a nylon matrix Gibson has shown that the entry pressure drop through a moulding machine nozzle has a minimum at less than an included angle of 40°. This appears to be most pronounced at high flow rates, with the pressure drop almost independent of entry angle at lower flow rates. Corscadden (5) has reported an increase in entry pressure drop with entry angle between 60° and 140° for long glass fiber in polypropylene using a ram extruder, with a maximum at about 120°, and with a minimum at less than 40° using an injection moulding rheometer at 5000 sec^{-1} shear rate. Some effect of the die diameter has been found with dough moulding compound (DMC) materials (4), but the effect of convergence ratio from the feed barrel diameter is unknown. All reported data are in a mixed shear and stretching flow regime at high shear rates. These observations relate to an imposed die taper entry configuration and this may differ from the natural die entry angle which the material follows in a 180° entry angle.

The extreme anisotropy of the feedstock provides the opportunity to measure along the fiber and transverse components in a defined geometry of flow such as a parallel plate rotational rheometer. With both steady shear and dynamic modes available, this provides a more fundamental characterisation and may allow rules for combining various sources of data for this type of material to be explored.

Since these compounds are used exclusively for injection moulding of engineering components, the type of flow which is characterised in this study is likely to be afflicted with pressure fluctuations and granule memory effects on a level which will not be as dramatic in commercial operations when the material will be plasticised on melting.

In commercial applications, materials are employed with a fiber loading (in weight %) from 30 to 60%. The fiber characteristics always dominate the mechanical properties. The influence of processing techniques and microstructure on the mechanical properties are addressed in the parallel study of this working party (6). The microstructural characterisation of these materials has been addressed for this family of materials for fiber length, orientation and dispersion by previous workers (7, 8, 9, 10, 23), however there has been little investigation into the passage of these materials through convergent flow.
Fiber length attrition is reported to be brought about predominantly by the screw preplasticisation in the injection moulding machine (7). Secondary attrition processes do occur at high shear rates which are of less significance.
Fiber orientation and dispersion play a far greater role in the flow characterisation. There is no clear picture of the mechanisms of how these fiber composites pass through flow constrictions with minimal fiber attrition which is evident from the dramatic melt fracture which occurs on elastic recovery of the fibres during die exit.
The determination of fiber orientation for these has been approached by a number of workers using image analysis and image processing from polished sections taken through moulded components and flow channels (8, 9, 10, 23). In a section through the composite, intersected fibres appear as ellipses which are light against a darker matrix background. These fields of view are converted into binary images by image processing. The orientation of the fibres can be determined from the angle of the major and minor axis of the ellipse relative to fixed reference axes in three dimensional space. It is customary to set the predominant flow direction as the X-axis in simple geometries. In mould filling studies, in a rigid fiber system, the fibres tend to be aligned by shear forces on entering a die and misaligned (relative to the flow direction) upon divergence. This gives rise to the classical 'fountain flow' mechanism, associated with the advancing flow front in mould cavities (11).

The active participants in this collaboration are identified in the text as follows:

Laboratory	
1	BASF Aktiengesellschaft, Ludwigshafen, Germany.
2	Solvay Central Lab., Bruxelles, Belgium.
3	ICI Materials, Wilton, UK.
4	Shell Chemical Research Centre, Louvain-la-Neuve, Belgium.
5	DuPont de Nemours & Co., Engineering Technical Lab, Wilmington, USA.
6	Hoechst Celanese, Summit, USA.
7	Technical University of Denmark, Lyngby, Denmark.
8	National Research Council Canada, Quebec, Canada.
9	Hoechst AG, Kunststoff-Forschung, Frankfurt, Germany.
10	University of Karlsruhe, Germany.

1.1 MATERIALS USED IN THE STUDY

Materials were supplied by Verton, LNP inc. and were compounded into two granule geometries (10 or 5 mm length x 2.5 mm diameter) from the precursor pultrudates, illustrated schematically in Figure 1. The composites under study comprised a low viscosity (MFI 100 [g/min]) polypropylene homopolymer, reinforced by 40% by weight E-glass fibres of nominal 17 μm

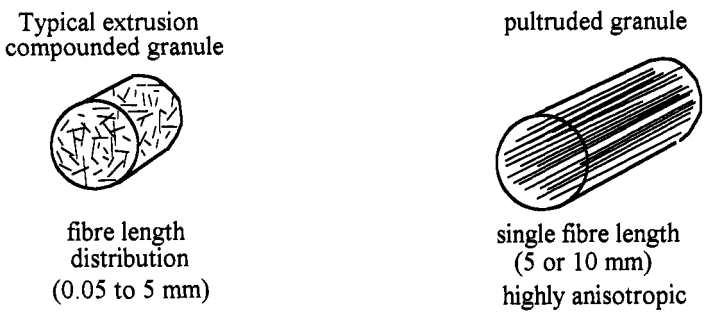

Figure 1. A schematic diagram showing the feedstock geometry and fibre alignment in the pultrusion compounded granules used in this study as compared to conventional extrusion compounded counterparts.

diameter. This system can be considered model materials since the formulations under study are not commercial, and were prepared with a view to eliminating some experimental difficulties in the characterisation. The two materials studied in this work follow the same nomenclature used through parallel papers (6) in this series, for 5 or 10 mm granules of glass fiber reinforced polypropylene; **PP/g 5** or **10**.

1.2 MATRIX CHARACTERISATION

The polypropylene matrix polymer has been characterised in order to demonstrate that this is a well behaved linearly viscoelastic polymer, and for background information for studying the composite properties (Laboratories 2 & 3).

The curve shown in Figure 2 illustrates the characteristics of this polypropylene material. There is some agreement between steady capillary flow, dynamic torsion and steady shear torsion. At 200 °C the shear viscosity is 700 Pa s at the lowest measured shear rate = 0.01 s^{-1}, the zero shear viscosity is likely to be in the 800 to 900 Pa s range.

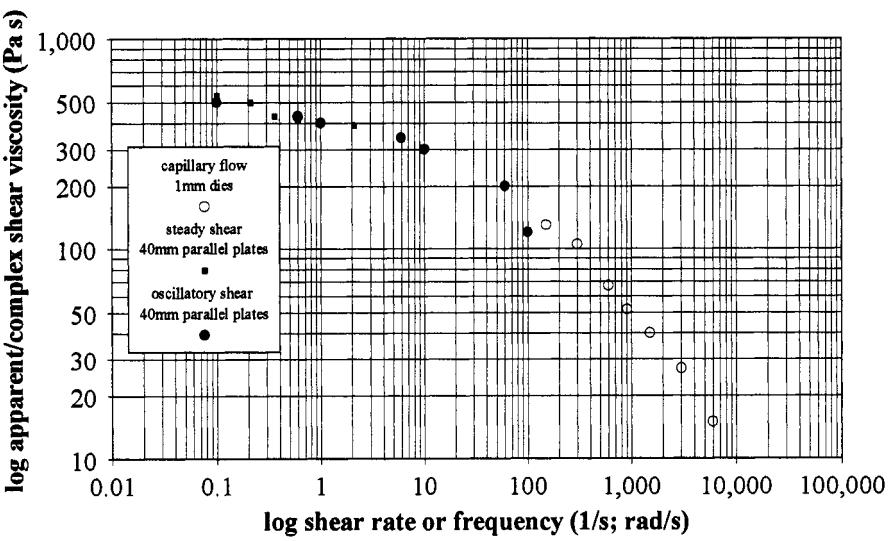

Figure 2. The flow curve for the matrix polypropylene homopolymer

The die entry pressure drop (P_L) as a function of die entry angle (total or included) is tabulated in Table 1 (these pressure drop values are for the dies described later and are not Bagley corrected). These data show that the unfilled system exhibits an inverse relationship between pressure drop and entry angle, but at each measured shear rate gives a similar pressure drop ratio value of around 2 for large (180°) to small angles (10°). The geometry for these measurements is shown schematically in Figure 3.

Die Entry Angle	36 s^{-1}	120 s^{-1}	361 s^{-1}	1203 s^{-1}
10°	1.7	3.3	6.2	11.4
20°	1.1	2.3	4.2	7.7
45°	0.8	1.6	2.8	5.5
90°	0.7	1.5	2.7	5.7
135°	0.9	1.5	2.8	6.2
180°	0.8	1.6	3.2	6.1

Table 1. The Die entry pressure (in bar) as a function of the total entry angle at different shear rates.

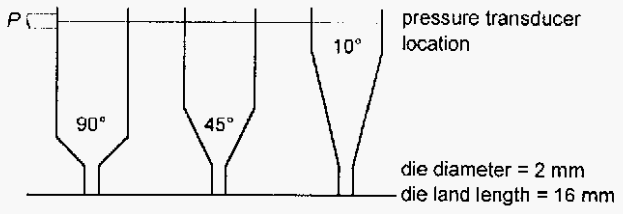

Figure 3. A schematic diagram showing differing die entry angles.

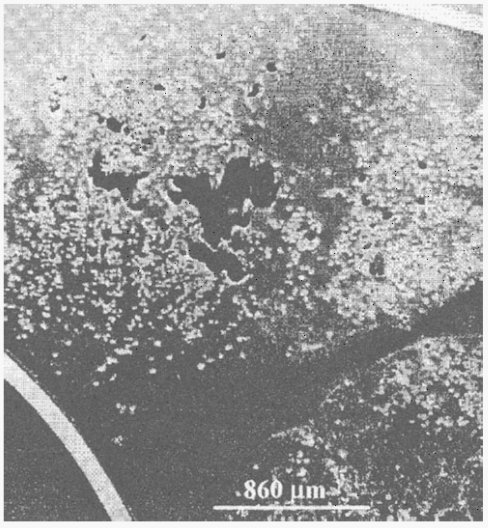

Figure 4. The fibre dispersion through the granule cross section, showing inhomogeneity.

1.3 GRANULE MORPHOLOGY

The pultrudate precursor is produced by a melt impregnation process which spreads and wets fiber rovings at high speed. The emphasis with such a compounding process is the efficiency of fiber wet-out i.e. the impregnation of the glass fiber roving by the polymer such that the glass surface and preparatory coupling agents interact with the polymer chains. The resultant fiber dispersion within the granule is often heterogeneous. This is illustrated in Figure 4, and is consistent with micrographs reported in commercial systems (12).

2. EXPERIMENTAL

2.1 STEADY CAPILLARY FLOW

The various stages of flow through a capillary rheometer are considered in turn, starting with die entry and finishing with die exit or extrudate.

2.1.1 Die Entry Flow

(a) Photomicrographs of Natural Entry Flow Angles

By interrupting the capillary flow experiment, when steady flow conditions have been established, by freezing the contents of the barrel suddenly, it is possible to carefully remove the die together with a plug of material originating from the die entry region of the barrel.

The die entry flow with an unconstrained 180° angle shows the fiber alignment in photomicrographs (Lab *H*) which illustrate a natural preferred entry cone (Figure 5). Sections cut along the flow axis yield a natural entry angle of between 40 and 60°, both for the capillary and in the converging path of the slit entry. While fibres tend to be aligned along the path of converging flow, the fibres in the recirculating zones appear to attain a more random or possibly circumferential alignment under the restricted flow condition with 20% of the barrel discharged (Figure 5). The recirculation is less well defined when the barrel has been discharged by 70% of its volume.

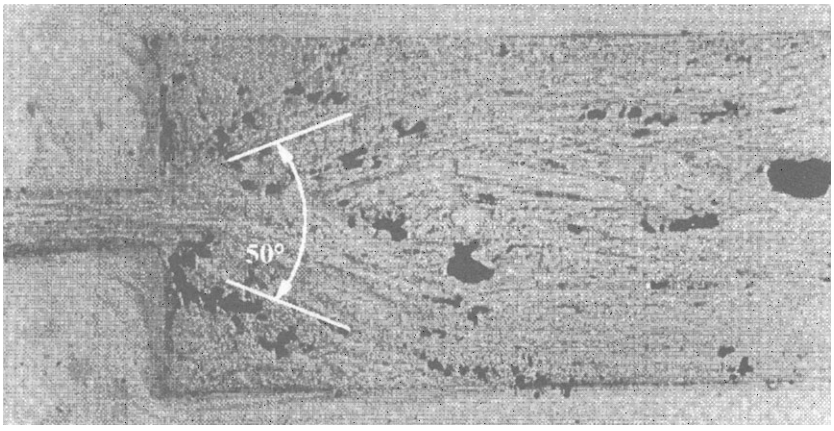

Figure 5. An optical micrograph showing a cross-section parallel to the extrusion direction. The streamlined and recirculation regions are clearly visible. (5x mag.)

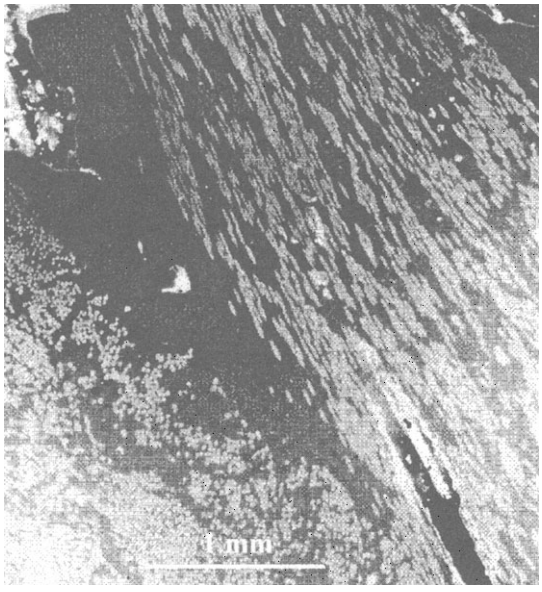

Figure 6. The interface between the die entry cone (streamline flow) on the right hand side and recirculation zone (left) shown at higher magnification using scanning electron microscopy. Some voids are present owing to the solidification taking place in the barrel. The lighter coloured glass fibres are shown against the darker polypropylene background.

Flow through a slit die shows random orientation of fiber bundles (or dispersed fibres) in the plane of the slit. It is noteworthy that despite two degrees of freedom in the slit, fiber crimping in the plane of the narrow dimension is still evident on die entry.

Observations of two die entry regions (Laboratories 3 & 6) has revealed that the natural convergence cone was also asymmetrical. The magnitude of the entry angles agrees with observations of previous workers (1) (approximately 50°) as shown in Figure 5 and 7. The micrographs show local fiber fraction variations in the entry funnel which relate to the dense fiber packing associated with these materials. In a capillary rheometer fiber bundles have experienced no plasticisation to randomise the fiber orientations of the granule history. The granules were melted by thermal conductivity alone. This has to be kept in mind if our data are compared with studies by previous workers, most notably Gibson, whose observations were made on well preplasticised materials.

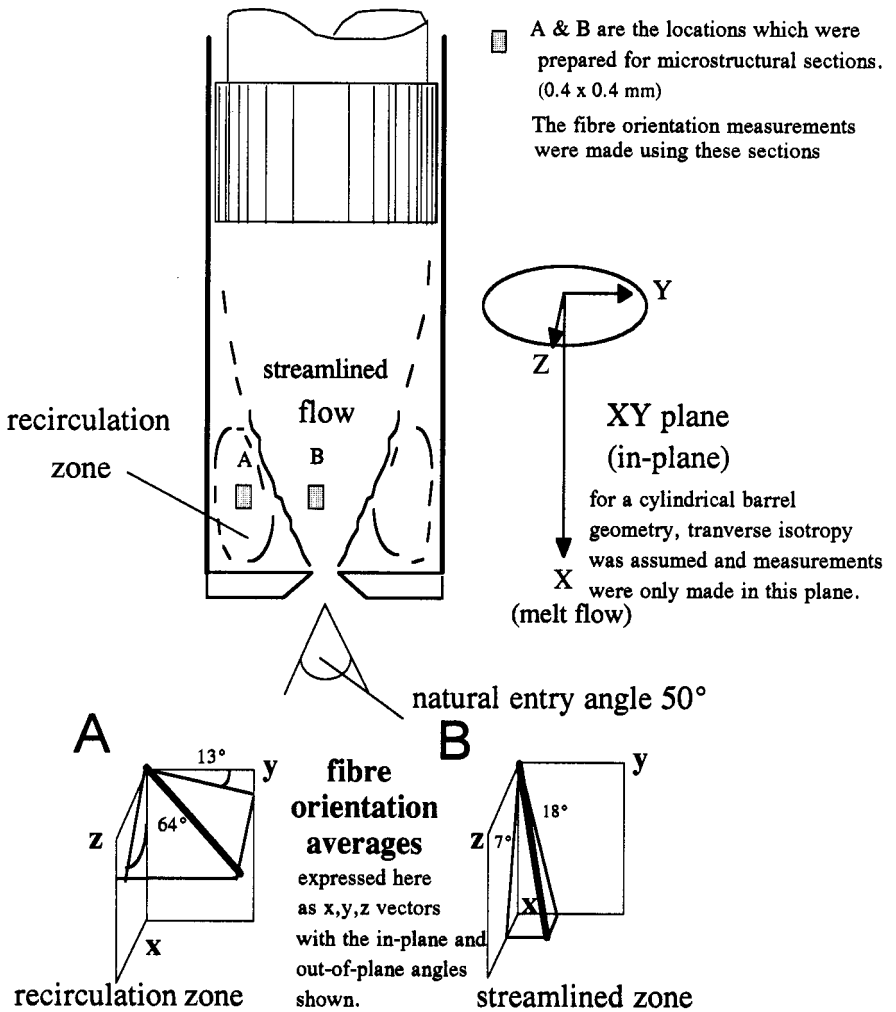

Figure 7. A schematic diagram shows the fibre orientation measurements made from the micrographs. The representation is for a cylindrical barrel with circular dies.

In order to quantify the streamlined and recirculation zones, the average fiber orientation angle relative to the die axis has been measured (Figure 7) using image analysis techniques (8,9,10). There is a significant difference in fiber orientation between the convergent flow funnel and the recirculation zones. The transition between the two regions is quite distinct with an abrupt transition (compare with Figure 6). The oriented fibres in the streamlined entry region have an average 7° in-plane angle and lie out-of-plane by 18°. The recirculation zone fibres are, on

average highly misaligned (13° in-plane, 64° out-of-plane). This latter observation is consistent with the recirculating fibres lying in a circumferential arrangement. It has been reported that there is an additional component of flow along this circumference of the barrel which occurs in the recirculation process (13). This would increase with increasing shear rate and would result in a component of rotation to the system on entering and exiting the die. Extrudates which exhibit a helical character have been noted by numerous workers.

(b) Pressure fluctuations

In these materials a dramatic pressure fluctuation is almost an intrinsic feature. Fluctuations in the zero length die pressure drop magnitude was around ± 50% with larger die entry angles from 135° to 180° (Laboratories 2, 3, 4 & 9). An example of the pressure readings obtained at a shear rate of 120 s^{-1} is shown in Figure 8 (Laboratory 4), the average pressure values were well defined. Each laboratory attempted to take the best averaged readings from their experiments, either by adapting their experimental techniques or utilising analytical software to give statistically significant information.

There is general consensus that at constant shear rate, large pressure fluctuations, typically greater than ± 25%, with no true equilibrium steady pressure at any time are observed. When data are obtained at constant stress in a gas pressure rheometer (Laboratory 1), the output extrusion rate fluctuates instead. In ram extrusion, the output rate is observed to vary correspondingly with the recorded pressure drop fluctuations.

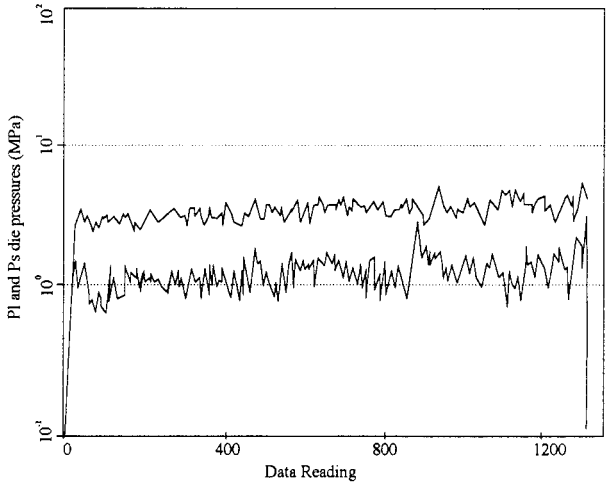

*Figure 8. Typical pressure fluctuations for a long (L/D=20) and short die (L/D=0). The longer die exhibits higher pressures as expected, but has a lower variation (**PP/g 5** at 200 °C).*

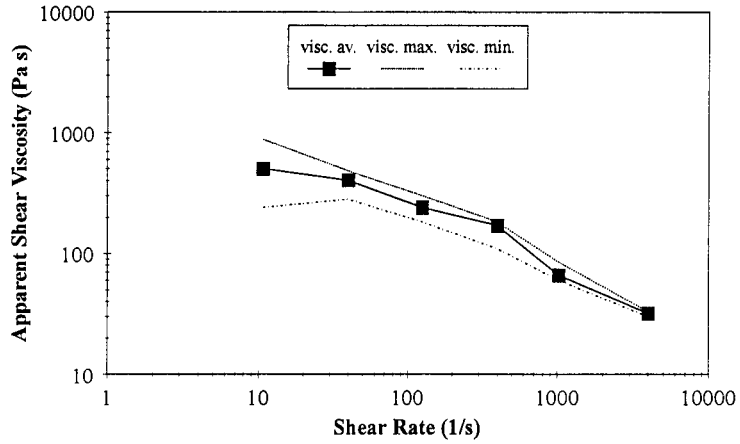

Figure 9. The corresponding data used to give a mean apparent shear viscosity together with an upper and lower value calculated from the varying pressures.

The relative pressure fluctuations are greater with short dies (L/D = 0) than with L/D = 20 for example as shown in Figure 8 (Laboratory 4). Furthermore, the pressure fluctuations tend to decrease, as a percentage of the mean pressure, when the shear rate increases. This is clearly shown in the accompanying viscosity variation plot in Figure 9 (Laboratory 4) and is confirmed (Laboratories 3 & 9) as a general trend. If material is passed through the capillary rheometer a second time, the pressure fluctuations are seen to decrease, this is the subject of a more extensive work programme by this IUPAC Working Party (24). This would be more representative of the condition in a processing situation and will be the subject of ongoing work by this study group. As with die entry angle, the pressure fluctuations are greater for **PP/g 10** than with **PP/g 5**.
The pressure fluctuations from slit die measurements (Lab HC) were recorded and analysed statistically. These show periodicity as discussed for the circular die geometry data for which there is significantly more data available. Interestingly, pressures recorded in the barrel could be compared to those recorded at a location within the slit die at a point closer to the exit of the slit. The pressure extrema are correlated (Figure 10).

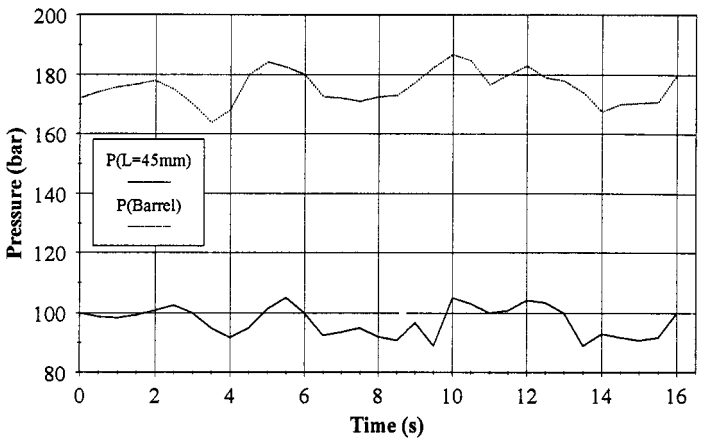

*Figure 10. The corresponding presssure fluctuations from above and within a slit die (**PP/g 10**, slit die 100 x 10 x 1 mm, shear rate = 500 s^{-1}, temperature = 200 °C).*

sample location	*Extrusion shear rate (s^{-1})*		
	38.4	**120**	**1,200**
beginning	22.2/27.3 32.1/33.8 36.0/43.2	35.8/38.3 43.9/45.2 47.3/53.9 54.3	23.6/28.0 34.0/38.8 44.0/44.1 44.5/48.4
middle	39.2/39.3 39.6/40.7	40.7/43.7 44.7/44.9 45.2/45.9	38.1/41.1 42.0/43.8
end	33.8/41.6 42.2/48.4 50.9	36.1/36.5 39.2/42.9 45.6/52.3	36.1/38.9 40.7

*Table 2. Showing the glass fiber content (%wt.) as a function of time and shear rate for material **PP/g 10**.*

Analysis of the extrudate fiber fraction has been recorded by thermogravimetric analysis (TGA) by oxidation at 500 °C and correlated with shear rate and the stage of the experiment (Laboratory 4) and is shown in the table below. The glass fiber content is shown as a function of shear rate for 2 mg samples (corresponding to approximately 2 cm length of extrudate). The measurements were made at the beginning, middle and end of the extrusion of the barrel volume.
The dramatic fiber fraction variability (from 25% to 50% by weight) seen here must have its origins in the die entry region and is clearly a dominant effect in causing the large pressure fluctuations. The variability is similar across shear rates of 38 to 1200 s^{-1}. However, the fiber

fraction appears to be more stable and closer to the nominal fiber loading of the material in the middle of the extrusion run (steady state conditions) than either at the beginning or the end.
The pressure surges have also been monitored whilst observing extrudate velocity. Not surprisingly, these two parameters are linked and occur at a characteristic frequency. Figure 8 and 10 shows the characteristic frequency at which these pressure fluctuations occur. This has been shown (Laboratory 10) to correspond to the fiber entrance time into the die convergence. This argument is further developed in the discussion.

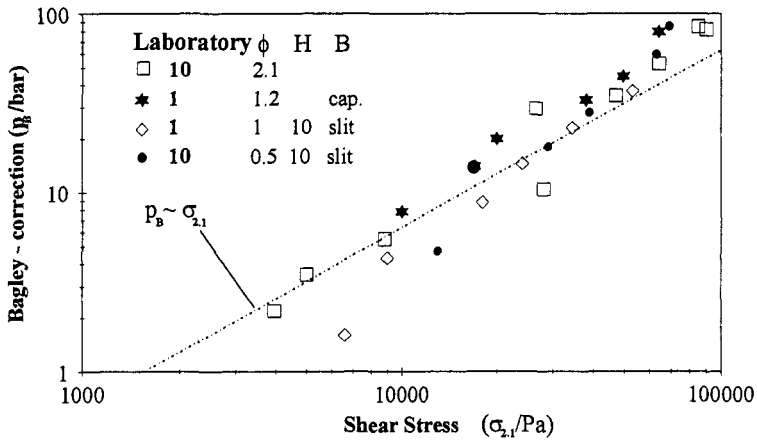

*Figure 11. The Bagley correction pressure (P_B) correlation with the shear stress showing good agreement between different laboratories and between slit and capillary dies. (**PP/g 10** at 200 °C).*

(c) Entrance pressure

An increase in uncorrected pressure drop (P_L) with entry angle was found (Laboratory 2) between 10° and 135° at 6 sec^{-1} shear rate, (assuming a die of L/R = 1) approximates to entry pressure (see Table 3). This is confirmed at 60°, 90°, 120°, 160° and 180° entry angles up to a shear rate of 400 sec^{-1} for **PP/g 10** (Laboratory 3).
The pressure increase with angle is greater for **PP/g 10** than for **PP/g 5**. The Bagley die entrance pressure drop (P_B) with a 180° entry die is also greater for **PP/g 10** than **PP/g 5** (Laboratories 1 & 9).

In contrast to this behaviour, a decrease of this Bagley pressure drop term with increasing entry angle has been shown for the polypropylene matrix (Laboratory 2) as shown in Table 1. The dramatic increase in extensional viscosity reported which is associated with a natural die entry cone and brings about oriented fibres entering the die, will be responsible for this.
This behaviour is shown to converge for both circular (Laboraties 1 & 10) and slit dies (Laboratory 6). It has been shown (Laboratory 10), that the Bagley correction pressure (P_B) increases proportionally with the shear stress (σ_{12}) and this is illustrated in Figure 11 by the broken line.The data plotted gives good agreement - even between circular and slit dies (Laboratory 6). It should be noted that in purely viscoelastic materials the Bagley pressure (or elastic pressure loss $\Delta P_E = P_B$) increases with shear stress faster than the 1st power.

entry angle (°)	*Pressure (MPa) 5 mm length material*	*Pressure (MPa) 10 mm length material*
10	0.1	0.15
20	0.15	0.2
45	0.2	0.25
90	0.33	0.4
135	0.3	0.6

*Table 3. The die entry pressure as a function of the total entry angle at shear rate 6 sec^{-1} using the same 2 mm die geometry shown in Table 1 (*Laboratory 2*).*

2.1.2 SHEAR VISCOSITY FUNCTION $\eta(\dot{\gamma})$

In Figure 9 the shear viscosity function has been plotted for a range of shear rates using the average pressure readings (solid lines) and considering the upper and lower values of the pressure fluctuations (this data was Bagley corrected using the average pressure drop values (L/D=0)) (see Figure 9).

Four laboratories provided viscosity - shear rate or viscosity function - shear stress data as shown in Figure 11. Two additional laboratories were of the opinion that the lack of a true pressure equilibrium, and some evidence of possible separation of the fiber and matrix polymer did not justify the presentation of quantitative viscosity data. Preferential extrusion of matrix was noted (Laboratory 7) at very low shear rates. Viscosities do not exhibit any trend as a function of geometry. Geometries are collated in Table 4.

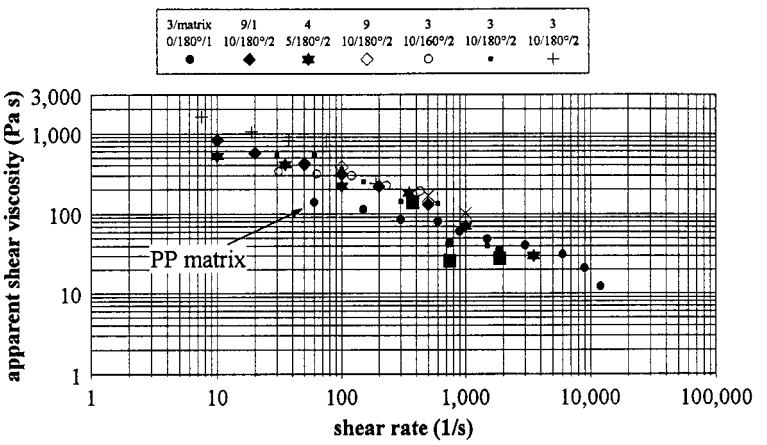

Figure 12. The correlation between laboratories for apparent shear viscosities from capillary flow.
*(**Nomenclature**: laboratories 3, 9/1, 4 etc. Die geometries given as die length/entrance angle/diameter)*

participant **(Laboratory)**	***geometry employed*** **(capillary die diameter; barrel diameter; entry angle)**	***10 mm material viscosities recorded (Pa.s) [shear rate in the range 75 to 150 s^{-1}]***
1	1.2 mm; 12 mm; 180°	380 [125]
3	2 mm; 15.5 mm,;30-180°	297 [120]
4	1 mm; 12 mm; 90°	200 to 320 [100]
6	slit die(H/B=1/10); 12 mm; 180°	340 [100]
7	2 mm; 16 mm; 90-180°	305 [100]
10	2.1 mm; 15 mm; 180° slit die(H/B=0.5/10); 15 mm;180°	250 [120] 250 [80]

Table 4. Viscosities measured using different experimental set ups.

Shear viscosity correlation between laboratories, shown in Table 4 and Figure 12 is good. Particularly taking into account the nature of the materials and the pressure fluctuations. The viscosity - shear rate data from each laboratory coincides with at least one other laboratory at some part of the shear rate range in spite of the range of instruments and geometries employed across the work group. There is a trend for **PP/g 10** to have higher shear viscosities than **PP/g 5**. The separated die entry pressure data, P_o as a function of shear stress also shows the trend for **PP/g 10** data to be higher (see Table 1) reported by Laboratory 10.

In slit die measurements, the data (measured only for 10 mm length feedstock) correlates well but consistently fall slightly below the circular die data (Laboratory 6). The slit die data is included in Figure 11, in which all data is plotted together. The slit die data is taken from the linear regression of the output from three internal transducers.

2.2 DIE EXIT FLOW

The form of the extrudate is shown for a range of conditions (Laboratory 10) in Figure 13. The extrudate surfaces tend to be partially or wholly disrupted with individual fibres or groups of fibres visible, as shown for **PP/g 10**.

Further, there is a clear indication that more disruption of extrudate correlates with greater pressure fluctuation for the **PP/g 10** compared with **PP/g 5**.

The larger the die entry angle, the greater is the tendency for disturbance of the extrudates, leading to exposed fibres. Furthermore, there is a tendency, which is not conclusive, that a shorter die land results in more disruption of the extrudate. There is insufficient information from a single common geometry to assess the effect of shear rate. The onset of melt fracture at low shear rates was noted by one participant (Laboratory 7). The influence of entry angle and land length on the extrudate condition appears to be consistent with geometrical effects on classical melt fracture*, particularly as the best extrudates were from entry angles of 45° or less with **PP/g 5**. (*Classical melt fracture has its origins in stick-slip effects or helical vortex occurring within the die.)

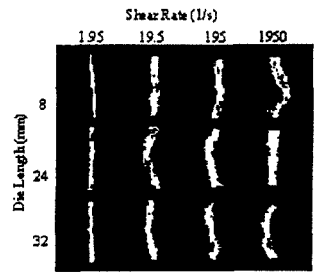

*Figure 13. The extrudate appearance for a range of shear rates (**PP/g 10** at 200 °C, die diameter = 2.1 mm).*

2.3 SQUEEZE FLOW

Squeeze flow measurements were made to obtain information on the flow of this material in a different configuration. The deformation is applied in compression in a direction perpendicular to the fiber axes (i.e. out-of-plane) and plays a substantial role in processing short fiber thermoplastic composites.

The material was compression moulded into 25 mm radius circular plaques to give random-in-plane fiber alignment.

The plaques were then squeezed at 190 °C at constant force (F) in a servohydraulic machine and the thickness (H(t)) monitored as a function of time (Laboratory 1). The technique assumes that if the viscous flow takes place at a constant viscosity, then the rim shear stress and shear rate can be calculated by the following relationship (22):-

$$\text{rim shear stress: } \sigma(t)_R = \frac{2H(t)F}{\pi R^3}$$

$$\text{rim shear rate: } \dot{\gamma}(t)_R = \frac{3\dot{H}(t)R}{H(t)^2}$$

$$\text{apparent viscosity: } \eta = \frac{\sigma_R}{\dot{\gamma}_R}$$

A plot of the similar type as that in Figure 11 and constructed for **PP/g 5** show a 40% higher apparent shear viscosity for the 10 mm fiber length material than the 5 mm counterpart.

This information also relates to the rotational testing since the geometry of the test is similar, and in preparing the sample for testing, a component of squeezing is required to attain the platen gap. It is noteworthy that the viscosity data obtained from squeezing correlate with the complex viscosity from the oscillatory shear data better than with capillary data. In Figure 14, the data is presented across an apparent shear rate range of 2 to 80 sec^{-1}, over which apparent viscosities ranging from 200 to 600 Pa s are noted.
In performing a squeeze test on this material, the test proceeds on the composite material until the gap reaches the point at which the glass fibres impinge on one another. This results in a sharp decrease of the squeezing speed and the data then becomes invalid. However, this does provide a useful insight into the geometric constraint in any squeezing component when either preparing the materials for other tests or in processing applications.

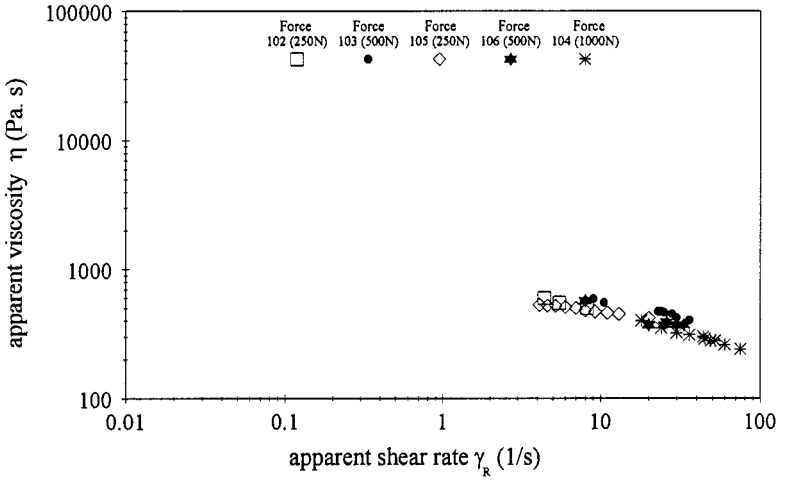

Figure 14. Squeeze flow results at 190 °C ***(PP/g 5).***

2.4 OSCILLATORY SHEAR

The rotational rheometry carried out to determine the dynamic viscoelastic fingerprint of the materials has been contributed by five contributors (Laboratories 1, 3,7, 8 & 9).

2.4.1 Non-linearity

Matrix Polymer: The polypropylene matrix polymer was essentially strain amplitude insensitive, measured up to a maximum or circumferential shear strain of 50%($\hat{\gamma}$=0.5), and was also thermally stable for at least 45 minutes at 200°C. The complex viscosity function (η^*) when plotted against angular frequency (ω) gives better agreement with steady shear viscosity (η) than as a function of shear rate. This is shown in Figure 2 using the Cox-Merz rule. As expected, there is good agreement of dynamic data with both the steady rotational viscosity at 0.1 sec^{-1} shear rate and the capillary flow data at 100 sec^{-1} .(Laboratory 3) (In steady rotation there is material loss and slip above 2 sec^{-1}).

Pultruded Compounds: The non-linearity was determined for strain amplitudes from 10^{-3} to 0.5. (0.1% to 50% strain). The ranges 10^{-3} to 1 at 3.14 rad/sec using cone and cone geometry (Laboratory 1); and 0.02 to 0.5 maximum strain using parallel plates at 1 rad/sec (Laboratories 3 & 8) and 10 rad/sec (Laboratory 8) are shown in Figures 15 and 16.
The composite materials exhibit non-linearity down to a shear strain of 10^{-3} in both 5 mm and 10 mm glass length variants. At higher shear strain and low frequency, more constant shear moduli G' and G" values seem to be obtained, although waveform analysis using Lissajous figures deviate from elliptical form indicating anharmonic waveforms at higher strains. However, there is no obvious drop in moduli values associated with the anharmonic waveform.

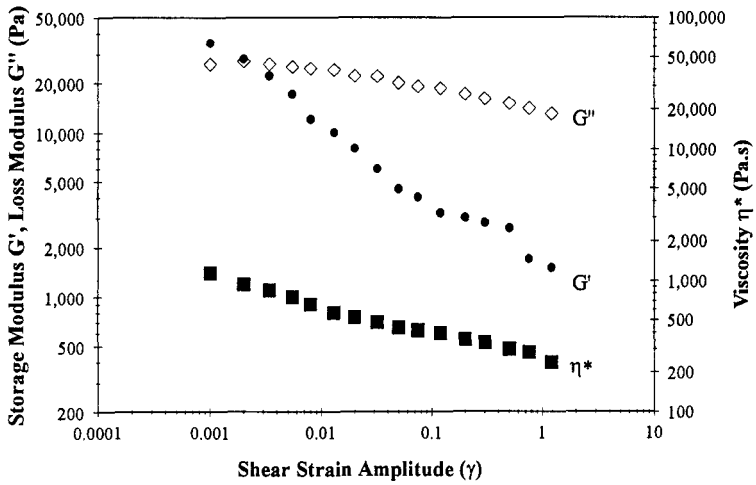

*Figure 15. The composite oscillatory shear behaviour at an angular velocity of 3.14 s^{-1} (**PP/g 10**), 200 °C.*

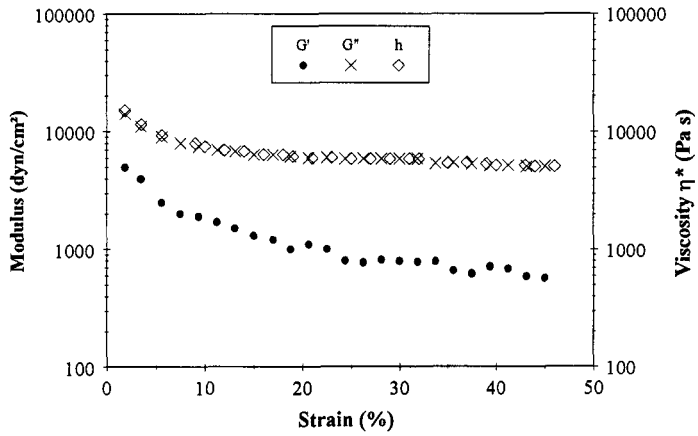

*Figure 16. The composite oscillatory shear behaviour at 1 rad/s for **PP/g 5**, premoulded sample, soak time = 12 mins, gap = 1.4 mm, 200 °C (note, for clarity some data have been offset)*

2.4.2 Comparison of Laboratories

The contributions of five laboratories show a clear variation which diverges most at the lowest frequencies, as shown in Figure 17. However, the variation is clearly not random, with the smallest shear strain data tending to be the highest in magnitude and the largest strain data the lowest. This should be independent of the waveform problems at the lowest frequencies.

2.4.3 Compressing the sample

There is an expectation that the fibre-fibre interactions in materials containing 40% by weight of fibres to be significant and furthermore, likely to increase as the composite is compressed between plates prior to analysis. Typically, a 3 g sample is compressed between 25 mm radius parallel plate platens to a gap of 0.9 to 1.5 mm. The variation of G', G'' and η^* , with 5 and 10 mm glass fibres is shown for these extremes in Figure 18 (Laboratory 7).

2.4.4 Yield stress

The low frequency plateau observed for G' and G'' which is shown in Figure 18 (Laboratories 1 & 8) infers that an apparent yield may impede the flow process. One method used to determine a yield stress from dynamic data is a modified Casson plot (14) of $G''^{1/2}$ versus $w^{1/2}$ (Figure 19). The intercept of the straight line gives ($G''y^{1/2}$), the mean shear strain ($\gamma = \left(\frac{\gamma}{2}\right)$). This gives a dynamic

yield stress of $\tau_y = G''_y$. Values vary for different data sets giving from 2.3 to 4.8 Pa for the 5 mm fiber length and approximately 4 Pa for the 10 mm fiber length.
Alternatively, an analysis for yield stress materials [15] predicts the product ($\gamma\omega$) as the effective shear rate for η^*. Extending this to effective shear stress in Figure 17 using mean strain for the parallel disc geometry, an upturn in η^*, asymptotic to the yield stress is clearly shown. Yield stresses from this analysis were approximately 4 Pa for the 5 mm fibres and 7 Pa for the 10 mm fibres variant.

2.4.5 Anisotropy

The polymer granules are highly anisotropic. Rotational tests were performed using compression moulded plaques which generally produce a random-in-plane fiber orientation. To determine the level of anisotropy in the rheology, granules were arranged between parallel plates and the fiber axis aligned either circumferentially or radially. Two laboratories found the complex viscosity and moduli to be higher for fibres aligned radially, with shear flow transverse to the fiber orientation. The small differences converged at higher frequencies as in Figure 20. A similar result was obtained for both fiber lengths with steady shear viscosity (Laboratories 7 & 9). Fiber orientation differences are unimportant at high strain rates as these are removed in performing the experiment.

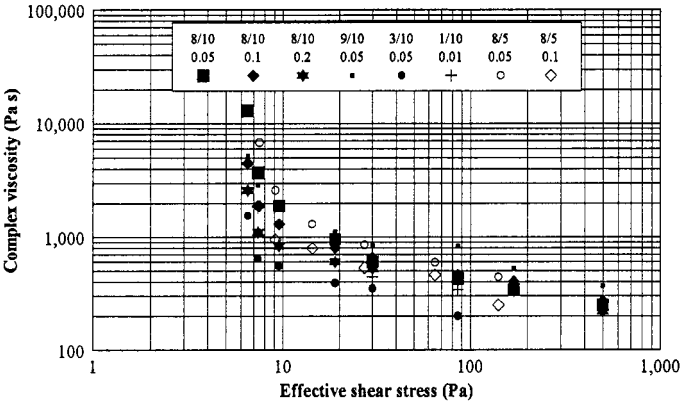

*Figure 17. A comparison of the oscillatory shear data collated for 5 mm and 10 mm fibre length composites. (**Nomenclature**: laboratories 8/10, 9/10, 1/10 etc. Strain %)*

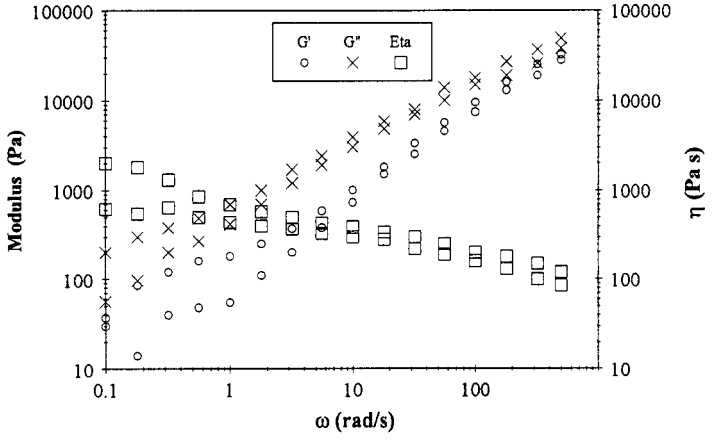

*Figure 18. The viscoelastic fingerprint for **PP/g 10** at two different gap thicknesses. The upper data represent a 0.9 mm gap and the lower 1.5 mm from the same mass of starting material.*

2.5 STEADY SHEAR ROTATION

Steady shear viscosities were determined if feasible, from 0.1 and 1 s^{-1} shear rate. They generally fall towards the lower end of the complex viscosity data are are included in the data contained in Figure 17.

The stresses are not small enough to assess whether there is a yield. (However, using a Casson plot of $\tau^{1/2}$ versus $\gamma^{1/2}$ would give yield stresses of 9 Pa and 11.6 Pa for the 5 mm and 10 mm materials respectively, which are higher than the dynamic data.

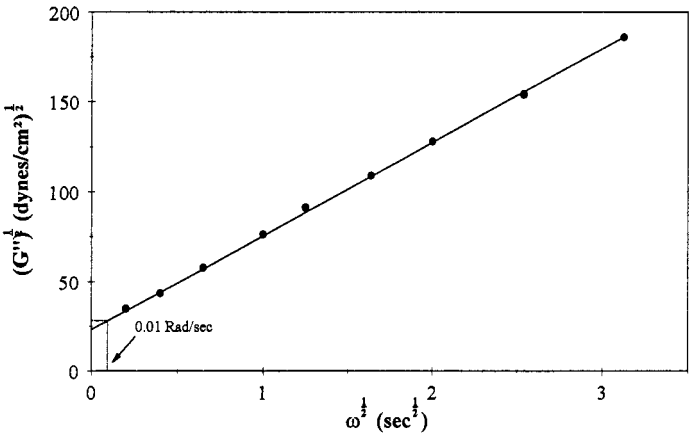

Figure 19. A modified Casson plot showing the extrapolated yield stress value (for PP/g 5).

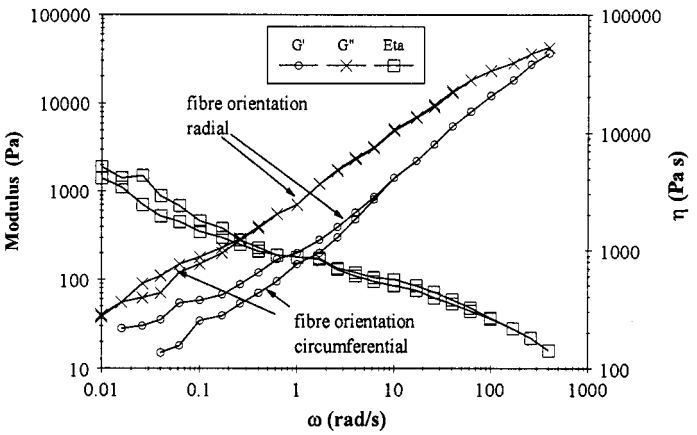

Figure 20. The anisotropy shown from oscillatory shear tests parallel and perpendicular to the fibre axis.

2.6 ELONGATIONAL VISCOSITY

The stress growth function (σ_{11}) versus time has been measured for the 5 mm material using a Rheometrics Extensional Rheometer (Laboratory 8). Samples were immersed in silicone oil (Dow 200) at 200 °C. The method is described by Munstedt (16). The elongational viscosity is shown as a function of time for three stretch rates ($\dot{\varepsilon}$ = 0.1, 0.3 & 0.5 s^{-1}) (see Figure 21). One notable feature of the data presented is the rapid drop in values at higher elongations, this is due to the problems in sample homogeneity especially in the molten state. The data does not converge across these stress rates because the material exhibits a yield stress. These values compare favourably with the data calculated for zero length die entry pressure drop (P_o) from the capillary rheometry using the Cogswell approach shown in Table 5.

The Trouton ratio is of the order of 200 which does not corresponds to the values reported by previous workers (2,5) which is given as being of the order of 30.

In relation to the extremely high values of Trouton ratio observed, it follows that the die entry angle dependence observed and reported shows the strong elongational component when these materials pass through restrictions. The irregularity of the extrudate, which decreases when the entry angle decreases agrees with this phenomenon. A fiber length reduction similarly improves the regularity of the extrudate, and clearly the high Trouton ratio would be reduced as the average fiber length decreases. The extrudate appearances are shown in Figure 22.

apparent shear rate (s^{-1})	*apparent shear viscosity (Bagley corrected) (Pa s)*	*transient extensional viscosity (kPa s)*	*Trouton ratio*
29.6	550.4	296.4	538.9
59.2	548.7	104.3	190
98.7	367.9	90.4	245.7
148.1	252.9	53.6	211.9
296.2	144.3	70.3	487
592.3	135.5	31.6	233

Table 5. Calculated transient extensional viscosity values from a Cogswell convergent die approach. These data correlate well with the Rheometrics RER direct extensional data shown in Figure 21.

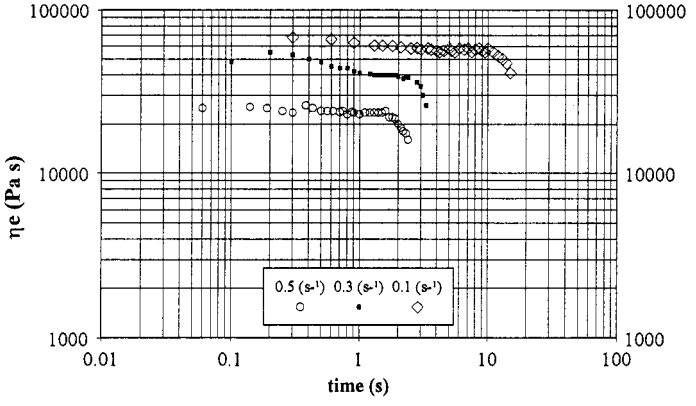

*Figure 21. Elongational viscosity measurements made using an Rheometrics RER rheometer **PP/g 5** for different stretch rates as indicated.*

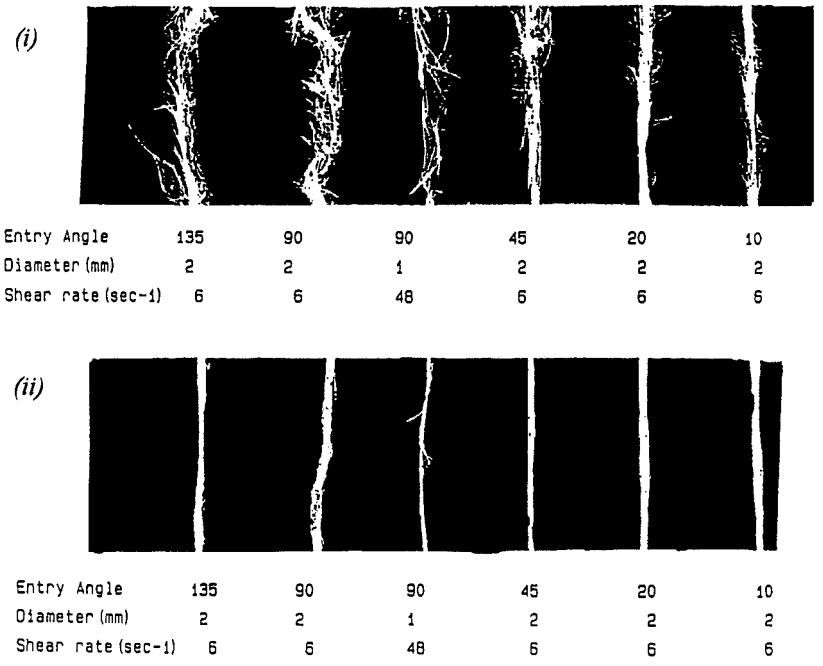

*Figure 22. The dependence of die entry angle on the appearance of the extrudates, i) **PP/g 10** and ii) **PP/g 5** both at 200°C.*

3 DISCUSSION

3.1 Material characteristics

The characterisation of the polypropylene polymer matrix was undertaken in order to elucidate the behaviour of the composite. The data presented in Table 1 show the die entry pressures determined for a range of die entry angles in capillary flow. The tensile flow component in the entry region which arises as the entry angle increases seems to be influential, and this could be explained by the die convergence extending the distance of influence. However, since the smaller dies have a reduced average cross sectional area, this may be attributable to a viscous effect arising from the greater resistance to flow of the differing entry cones. It has been suggested that if the reducing die entry pressure with increasing entry angle were related to an extensional effect, there ought to be a quadratic dependence on the entry angle because of the P_o^2 term in calculating elongational viscosity.

The characteristics of the feedstock of these materials are atypical for injection moulding or extrusion processing. While the form of the feedstock contains a discrete fiber length distribution which corresponds to the cylindrical granule length, the fiber dispersion (i.e local fiber fraction as seen in Figure 3) through the diameter of the cylinder varies considerably. The close, parallel fiber packing in the granule cylinders will have some significance in the context of flow phenomenon. It is clear that the fibres cannot be disrupted by shear applied normal to the fiber axis other than to cause fiber fracture, and that in the absence of plasticisation where forces are of sufficient magnitude to cause fiber fractures, the fibres will tend to be grouped closely together even after substantial rearrangement in a ram extruder barrel. There is a considerable microstructural evidence from hypothesis this work and also from that of previous workers to support the proposal that the fiber orientation and dispersion of fibres passing through the die are unique to long fiber thermoplastic compounds.
The die entry region micrographs illustrate that fibres flow in isolated packages of length L, or 'domains' (a term first used by Gibson (1) in relation to these materials).
The existence of a natural entry angle and the well established recirculation zones has also been reported by Gibson. However, the fiber orientations within each region has not hitherto been measured. The degree of orientation mismatch between these two regimes indicates that flow is probably circumferential as well as radial in the vortices.
This type of flow promotes a number of possibilities which may be responsible for the pressure fluctuations commonly observed:-

- local variations in fiber orientations entering the die.
- fiber fractions variations which cause either temporary die blockage or polymer filtration effects.
- interaction between the streamlined and recirculation zones in the die entry region.

To summarise the rheological behaviour, the low molecular weight polypropylene homopolymer matrix acts as a well behaved simple viscoelastic fluid. However, the addition of long fibres in a semi-ordered structure, with a degree of chemical coupling forming the interface between polymer and fiber transforms the fluid into a highly anisotropic non-linearly viscoelastic material.

3.2 Capillary flow

In the die entry and exit processes, three distinct morphological effects have been observed which distinguish these materials from the behaviour of most filled thermoplastics : i) the fiber orientation in the die entry vortex and streamlined flow regions, ii) a huge variability in fiber fraction in the extrudate, and iii) the extraordinary extrudate appearance.

It has been reported that these materials are difficult to work with because of the extreme anisotropy and the local orientation variations and rapidly changing morphology in the region of the die entry in capillary flow measurements.

The pressure drop values exhibit a lack of a true equilibrium over a short timescale i.e. the pressures are very noisy with scatter up to ±25%, but over a long period for a given shear rate, data can be analysed to give a mean from which the apparent viscosity can be calculated. In spite of objective difficulties a consensus has been reached among laboratories. This data is presented in Figure 12. In performing the capillary measurement at any given strain rate, the need to define an analysis protocol was considered by the collaborating laboratories (such as establishing a satisfactory pressure equilibrium in a period less than 30 seconds), however this was eventually dismissed and a consensus was reached whereby each laboratory would determine their own mean values for pressure drop values taken over longer period of extrusion, and this resulted in reproducible data.
The rheometer size is not significant. In the measurements made in this project, capillary rheometers ranged from 10 mm to 20 mm in barrel diameters and entry angles from 30° to 180°. All produced comparable results.

There is some division between contributors, they fall into two schools of thought. The first school suggests that the die entry angle dependence indicates a strong elongational viscosity influence from the observations made by Gibson arising from the presence of very long fibres. The second school suggests that the die entry effect is purely a viscous effect associated with the increasing average entrance cross section and the fiber bending forces superimposed. At low entry angles the fibres can be aligned by consuming less dissipation energy than at higher entry angle cones. *Each of these possibilities are equally valid and are worthy of further investigation.*
The increase is consistent with the dependence found by Gibson using a moulding machine at higher shear rates (1).
Results with the polypropylene matrix show the opposite i.e. a pressure fall with increasing angle. This behaviour must be linked to the pronounced die entry cone, i.e. observations made for the composite which is generally not encountered in an unreinforced high MFI polypropylene homopolymer. Increased recirculation vortices tend to be observed with broader molecular weight or branched polymers.
Two possible factors contributing to the die entry cone and the entry angle effect on the pressure drops are:- Firstly, the differing elongational flow behaviour and secondly, the melt elasticity. On the one hand, if this effect may be due to the differing elongation viscosity component between the composite and the matrix polymer, the high extensional viscosity in the composite is responsible for the pronounced die entry cone observations. The effect of enhanced fiber orientation and minimum fibre-fibre and fibre-wall interaction has also been suggested.
On the other hand, whilst the presence of such extraordinarily long fibres increases the stored elastic energy, whilst the presence of fibre-matrix coupling agents will promote a greater long range network structure in the polymer (akin to a broader molecular weight) and increase the overall elasticity of the melt. A comparison of the matrix and composite elastic components reveals this effect.

Pictorial evidence of the natural entry flow angle in two geometries, capillary and slit, indicates that an angle between 45° and 60° is most probable. This corresponds well with the Gibson minimum pressure entry angle (1). This is a much smaller natural entry angle than that found for short glass fiber in polypropylene (17) which endorses the higher elongational viscosity in this system.

Non-uniform fiber distribution in the feedstock granules has been suggested as a source of pressure fluctuation. This seems unlikely because measurements on reworked material from extrudates show similar fluctuations.
When a geometrical constraint is imposed on this heterogeneous material, it is clear that the local variations in fiber fraction and oriented fiber packages are aligned in a non-ideal fashion arising from being tumbled at random into the extruder barrel on charging. Pressure fluctuations might therefore be expected if die blockage followed by an abrupt clearing or unblocking, corresponding to pressure build-up and loss. However, actual blockage is seen in small diameter dies but the extrudate velocity is normally steady under test using a 1mm or 2mm die diameter. It is proposed

that pressure fluctuations arise by fiber rearrangements in the die entry region and the micrographs presented in this work support this view (Figures 5 and 6). If fibres are pultrusion compounded into the granule morphology shown in Figure 1, we can calculate an approximate frequency of rearrangement by comparing the aligned portion of each granule that can pass through a given die and this will lead to the number of rearrangements for each granule before it can pass through the die entirely.

3.3 Frequency of fiber rearrangement

One approach has been to calculate a characteristic time (T_e) from the fiber length (l_f), the volumetric flow rate (Q) and the extrudate velocity ($\bar{V}$) which is the volumetric velocity within the die ($\bar{v}=\frac{Q}{A_d}$), and relates to the mean entrance velocity into the die and is of course proportional to the apparent shear rate $\dot{\gamma}$ (Laboratory 10).

$$T_e = \frac{l_f}{\bar{v}}$$

The pressure fluctuation cycle frequency is proportional to the extrudate velocity and not the shear rate calculated from the piston speed.

The experimental evidence presented in this work shows that there is a significant fiber rearrangement taking place at the die entry which is reflected in the pressure fluctuations and the varying extrudate speed. This regime can be considered further by calculating the likely frequency of events. In order to simplify our model, we must assume a homogeneous dispersion of the glass fibres in the polypropylene polymer matrix. The material comprises 40% by weight fiber fraction (=25% by volume (V_f)); each granule contains 4,000 fibres of 17 μm diameter.
In streamlined flow, with all fibres perfectly aligned, the number of fibres which can pass through the die at once can be calculated by treating the situation as a 2 dimensional problem (this is not unreasonable because of the transverse symmetry of the granule geometry):-
The number of parallel fibres (of radius R_f) which can pass through a circular die (of radius R_d) at once is given by:

$$N = \frac{\pi R_d^2}{\pi R_f^2} V_f = V_f \left(\frac{R_d}{R_f}\right)^2$$

[in practise, R_f=8.5 μm; R_d=0.5 mm; V_f=25% volume. Therefore N=865; when R_d=1 mm, N=3460]

The entrance time for granules can be expressed as follows:

$$t_e = \frac{V_g}{Q} = \frac{\pi R_g^2 L_g 4}{\dot{\gamma}\pi R_d^2} = 4L_g\left(\frac{R_g}{R_d}\right)\frac{1}{\dot{\gamma}}$$

[R_g=1.25 mm (granule radius); R_d=0.5 mm (die radius); L_g=5 mm (granule length); $\doteq$100 s^{-1}. Therefore the entrance time t_e=1.25 s].
If it is preferred for flow to occur in domains of parallel fibres (as reported by Gibson (1)), then each granule (containing 4,000 fibres) must divide itself into approximately 4 parts to pass through a 1mm die. This 'partition factor' (X (the number of splits per granule)) is related to the frequency of granule events (that is the frequency of parallel packages of 10 mm long fibres entering the die) as follows:

$$f_e = \frac{1}{T_e} = \frac{X}{T_g}$$

[This frequency equates to approximately 3.2 s^{-1} for a 1mm die and 10 mm long fibres using the material under study.]

In a capillary test the volume flow rate (Q) through a capillary with a given radius (R_d) is given by the simple expression:-

$$Q = \frac{\dot{\gamma}\pi R_d^3}{4}$$

Across a range of shear rates ($\dot{\gamma}$) the granule 'packages' will take a given time to pass into the die, and in this time the granule must also divide by 4 (1 mm die) or 2 (2 mm die) times.
The table below illustrates the frequency of the rearrangement events for a range of operating shear rates calculated from this simple approach. [The volume of each granule = 3.63 x 10^{-8} m^3. The number of rearrangements per granule = 4.62 for 1 mm die (1.16 for a 2 mm die)].

shear rate (s^{-1})	**Volume flow rate (Q) ($m^3 s^{-1}$) (x 10^{-9})**	**Entrance Time (T_g) for a complete granule (s)**	**Rearrangement 'event' frequency (s^{-1}) [$f_e=1/T_e$] (for 10mm fiber length granules)**
10	0.98 (15.71)	37 (**9.24**)	0.13 (0.25)
100	9.82 (157.08)	3.7 (0.92)	1.25 (2.5)
1,000	98.2 (1570.8)	0.37 (0.09)	12.5 (25)
10,000	982 (15708)	0.04 (0.009)	125 (250)

Table 6. The rearrangement frequency calculated from geometric considerations (Figures in brackets are for 2 mm die).

Of course, in practice the mechanism for granule rearrangement is a more complicated 3 dimensional problem and as has already been described the die entry regions becomes established with a streamlined die entry cone and recirculating zones. Furthermore, three other key assumptions do not hold. Firstly, fibres do not enter the die with perfect alignment, the measured orientation in the streamlined flow area is not perfect and hence increases the likely number of rearrangements needed. Secondly, homogeneity is not upheld, and this is clearly shown by the range of extrudate fiber fractions determined by thermogravimmetric analysis; this could have the effect of either increasing or decreasing the number of rearrangements but will be constrained over a longer period to the nominal material volume fraction. The third consideration is due to the breakage of the brittle glass fibres which if abraded, crimped or placed under sufficient shear or bending forces will break. The presence of shorter fibres will help to fill in the interstices between the unbroken fiber packages and will reduce the number of required rearrangements.

Interestingly, it has been noted by more than one contributor that fibres congregate in a circumferential alignment at the bottom of the barrel in the recirculation zones. This suggests that it is energetically favourable for the recirculation to take place with the fibres flowing in this zone by presenting their full aspect ratio to the flow, which enables turning in the confined space without fiber crimping or breaking to occur.

3.4 Flow through the die

As for any material passing through a parallel sided capillary, the flow is established along the pressure gradient from the entrance to the exit. The velocity profile will tend to become a more plug flow profile as the shear rate increases. In long dies this allows a degree of relaxation to take place and this is illustrated by the reduced die swell effect shown in Figure 13. The extrudates shown will also be influenced by temperature effects on cooling and solidification for differing shear rates. For shorter or orifice dies, the opportunity for elastic recovery in the die is reduced and the extrudate expands energetically on leaving the die. In this case separate parts of the individual fibres or bundles may be present in die entry, land length and released from the die exit

all at the same time. This places additional constraints on flow and may be a further factor to be considered in the materials.
It has been noted that the extrudates contain variable fiber fractions and the volumetric flow rate through the die is not a constant.

3.5 Die exit observations

The nature of the extrudate form has been demonstrated in Figure 13. Fibres and bundles erupt from the die and produce a foamed appearance as elastic recovery takes place. This elastic energy is stored in the fibres and should not be confused with any relatively insignificant melt elasticity observed in the polypropylene melt.
In order to validate the fiber rearrangement calculations described earlier the pressure fluctuations have been further studied by relating the periodicity of these events to the extrudate velocity and appearance (see Figure 10). The determination of the extrudate velocity ($\bar{v}$) at any point through the die, and knowledge of the fiber length (10 mm)(L_O) allows the characteristic entrance time (t_d) to be calculated and this approach can now be compared to the fiber arrangement calculations.

$$t_d = \frac{L_o}{\bar{v}}$$

This characteristic time is obviously related to the shear rate ($\dot{\gamma}$). Figure 10 shows this calculated time period superimposed on the pressure fluctuation trace at a shear rate of 9.7 s^{-1}. The characteristic time of **3.9 s** is of similar magnitude to the **9.2 s** calculated by rearrangement for 10 s^{-1} in Table 6. Note: The extrudate velocity is not constant, but increases and decreases in proportion to the pressure recorded.
We conclude from this correlation that the rearrangement events and the time for each granule to be extruded from a given die are related. Obviously, the frequency of events (f_e) increases in proportion with the shear rate until the corresponding pressure fluctuations can no longer be resolved. This data convergence (pressure extrema) is shown in the viscosity curve plotted using the upper and lower pressure values in Figure 8 (Laboratory 2).
The agreement between the geometry calculation with both pressure fluctuations recorded and the die exit observations gives a measure of confidence in the fiber rearrangement hypothesis proposed.

It is clear that any rheological measurements of this composite system will be affected by microstructural factors. In real processes, these effects are less significant and the pressure fluctuations will be less dramatic. This will be due to the materials being subjected melting under shear and subsequent plasticisation, thereby dispersing the fibres into shorter lengths and fewer fibres in parallel alignment bundles. This consideration suggests that the fiber attrition mechanisms relate to the convergence ratio and shear rate imposed in the flow regime, which may seem an obvious point but may a provide useful criterion for designing gate and runner systems in injection moulds. For a given geometry, the rearrangement frequency can be calculated as shown; it is reasonable to assume that above 10 rearrangements per second, the fibres are physically incapable of moving into an aligned orientation and still pass through the die undamaged. Misaligned fibres will be crimped on entering the die and this will result in fiber attrition. The dies and runner dimensions on injection moulding machines are of significantly more generous convergences. However, shear rates are considerably higher (1000 to 100 000 s^{-1}).
The effective fibres aspect ratios can either be reduced by flowing as an agglomerated bundle, i.e. the fiber proximity is retained from the alignment in the granule, or are broken into individual fibres which can survive the spatial hindrance constraints and complex shear and tensile forces in their flow path. Bundles containing 30 to 100 fibres have been reported (2).
Intact fiber bundles are clearly visible in the extrudate which have passed through the die with considerable rearrangement but with little or no fiber breakage. Since it is these longer fibres

which impart the mechanical property advantages in moulded components it is of interest to promote and encourage the unhindered flow of fibres through die constrictions without unnecessary breakage.

It may be concluded that these materials give rise to measurement difficulties - due to the pronounced short time-scale pressure variations observed over a short time-frame, but that this feature is an inherent feature of their flow. If the precursor geometry is responsible for this effect by virtue of necessity for geometric reorganisation to pass through the die constriction, then enhanced flow may be derived through tailoring of the granule. Pressure fluctuations and hence extrudate disruption may be suppressed by a mechanism from the following list:-

i) fewer fibres in each 'package'.
ii) tailored inhomogeneity.
iii) finer fiber diameters.
iv) the presence of some shorter fibres to assist flow.
v) shorter granule lengths (as shown by comparing the 5 mm with the 10 mm material).

These issues pose numerous questions concerned with the possibilities for ordering or randomising during flow in the context of real processes. This subject will form the basis of the second project to be undertaken by this working party.

In particular, the nature of the extrudate and whether the extrudate emerges in a streamlined manner or is highly disrupted are important for mould filling situations. While the accepted injection mould filling mechanism is 'fountain-flow', which gives rise to the skin-core structures characteristic of fiber filled thermoplastics, the state of the in-flowing melt stream is not considered in any such model. The prevailing flow conditions will influence the fiber dispersion, length and orientation distribution and will dictate the preferred flow path. This may have more profound commercial significance.

3.6 Oscillatory shear

The dynamic measurements carried out either in parallel plate or cone and cone torsional geometries show a highly structured strain dependence The non-linear viscoelastic behaviour, with enhanced shear moduli G' and G" at lower angular frequencies suggesting a yield stress response, is sensitive to compression or squeezing of the specimen, which varies with both the plate separation or sample thickness and the residual matrix polymer to fiber ratio. Some spread of data among laboratories is therefore to be expected.

Treatment of these composites as yield stress materials using the effective shear rate according to Doraiswamy et al (15), and extending to effective stress (18), diminishes the deviations due to both shear strain and geometry (parallel plate mean stress, $\gamma_{mean} \approx \frac{\gamma_{max}}{2}$, and cone and cone true stress).

The indicated yield stresses (4 Pa and 7 Pa) may be compared with a value of 20 Pa (19) measured by the same method or by modified Casson plots, for a related polymer system, but taking samples with 25 mm and 50 mm long fibres from a continuous fiber composite.

Although this effective shear rate treatment rationalises the non-linear viscoelasticity, the values obtained agree neither with capillary nor with the steady shear rotational data. Owing to the extreme inhomogeneity in these materials, one explanation for the discrepancy in correlating the different rheological test techniques may be the local polymer rich layers which are found at the surface of the granule, surrounding the fiber bundles. These resin rich regions could translate to polymer rich wall layers in the parallel plate geometry. There is, however, much closer agreement with squeeze flow data (allowing for the slight temperature difference at 190 °C), obtained from a similar parallel plate geometry but with a radial steady flow regime. The steady rotational viscosity data unexpectedly fall within the spread of complex viscosities when plotted using the Cox-Merz rule.

Prediction of anisotropy in the composite rheology shows some agreement between oscillatory and steady shear flows, with the radial fiber orientation, i.e. transverse polymer flow relative to the fibres, having a slightly higher viscosity. The difference may not be significant when considered in relation to inter-laboratory and general measurement variance. However, the result is in accord with published data for composites (19,20), including a similar polymer and fiber system from a continuous fiber composite.

This study has concentrated on the material in it's feed stock form. However, the work has been extended to explore the modification to rheology properties as the material is processed and recycled (24).

4. CONCLUSIONS

i In spite of the unfavourable feedstock geometry in relation to capillary rheometers, reproducible data have been obtained by participating laboratories.

ii Long fiber reinforced thermoplastics exhibit high Trouton ratios which produce extreme small die entry angle cones and associated large recirculation zones.

iii The pressure fluctuations observed, are associated with fiber rearrangement events which produce dramatic re-orientation and fiber fraction variations in the extrudate. These pressure variations are an inherent feature of flow in these materials which can be considered a short timescale effect. Over a longer time frame, the die entry pressure drops can be viewed as a steady plateau happening.

iv The frequency of granule rearrangement (calculated from geometric considerations) correlates well with extrudate velocity and pressure fluctuation data. The pressure events which arise from fiber rearrangements occur at a frequency of approximately once per second at 100 s^{-1}.

v Increasing shear rates results in:- a) inhomogeneity (a more pronounced fluctuation in fiber concentration); b) combined thermal and elastic fiber recovery effects in the extrudate, and c) greater pressure fluctuation.

vi Finite length fiber thermoplastic composites are highly strain amplitude dependent in oscillatory shear measurements. This results in a spread of data from different laboratories. By using an effective shear rate approach the data can be coalesced.

vii Oscillatory shear data correspond to squeeze flow measurements. However, they show a poor correlation with the steady shear rotation and capillary measurements.

viii Yield stresses of 4 Pa and 7 Pa have been calculated for 5 mm and 10 mm fiber length composites respectively using a modified Casson approach.

5. REFERENCES

1. A G Gibson, Composites 20 1 (1989) p57.
2. A G Gibson, S P Corscadden, A N McClelland J Thermoplastic Composites 1 2 (1988) p136.
3. A G Gibson, Plastics and Rubber Processing and Applications 5 (1985) p95.
4. A G Gibson, G A Williamson, Poly Eng Sci 25 15 (1985) p 980.
5. S P Corscadden PhD Thesis University of Liverpool UK (1989).

6. A. Cervenka and P.S.Allan: Characterisation of finite length composites - Part I: Introductory paper, Pure Appl. Chem., submitted for publication.

7. R Mittal, V Gupta & P Sharma Comp. Sci. & Tech., 31 (1988) p295.

8. G Fischer & P Eyerer Proc. 44th Ann. Tech. Conf., SPE, p164 (1986).

9. S Toll & P-O Andersson Composites 22 (1991) p298.

10. A. Clark ICAM'91.

11. Z Tadmor J Appl Poly Sci 18 (1974) p1753.

12. R Bailey D R Moore I M Robinson & P M Rutter
Science & Engineering of Comp. Matls. 2 No.3 (1993) p171.

13. D Binding (private communication)

14. L A Utracki Polym. Composites 7 (1986) p274.

15. D Doraiswamy etal J Rheology 35 (1991) p647.

16. H Münstedt J Rheol 23 (1979) p 421.

17. G Akay J Non-Newtonian Fluid Mech. 13 (1983) p309.

18. D J Groves Composites 20 1 (1989) p 28.

19. D J Groves, A M Bellamy, D M Stocks. Composites 23 2 (1992) p75.

20. D J Groves, D M Stocks, Composites Manufacturing 2 3/4 (1991) p179.

21. G K Batchelor J Fluid Mech 44 3 (1970) p 419.

22. H M Laun, Makromol. Chem., Makromol Symposia 56 (1992) p 55.

23. G.J. von Bradsky, R.S. Bailey, A. Cervenka and G. Zachmann: Characterisation of finite length composites - Part IV: Structural studies on injection moulded composites, Pure Appl. Chem., submitted for publication.

24. W. Gleißle: Characterisation of finite length composites - Part VII: Rheology - part 2 , Pure Appl. Chem., in preparation.